



Evaluation of lateral barrier height of inhomogeneous photolithography-fabricated Au/n-GaAs Schottky barrier diodes from 80 K to 320 K

D. Korucu^{a,*}, H. Efeoglu^b, A. Turut^{c,d}, S. Altindal^e

^a Department of Material Science and Engineering, Faculty of Engineering, Hakkari University, 38400 Hakkari, Turkey

^b Department of Electric and Electronic, Faculty of Engineering Ataturk University, 25240 Erzurum, Turkey

^c Department of Physics, Faculty of Arts and Sciences, Ataturk University, 25240 Erzurum, Turkey

^d Department of Physics Engineering, Faculty of Sciences, Istanbul Medeniyet University, 34000 Istanbul, Turkey

^e Department of Physics, Faculty of Arts and Sciences, Gazi University, 06500 Ankara, Turkey

ARTICLE INFO

Available online 9 April 2012

Keywords:

Schottky barrier inhomogeneity
Photolithography
Flat band barrier height
To anomaly
Temperature dependence
Ideality factor
Barrier height
Effective barrier height

ABSTRACT

In order to evaluate current conduction mechanism in the Au/n-GaAs Schottky barrier diode (SBD) some electrical parameters such as the zero-bias barrier height (BH) $\Phi_{bo}(I-V)$ and ideality factor (n) were obtained from the forward bias current–voltage ($I-V$) characteristics in wide temperature range of 80–320 K by steps of 10 K. By using the thermionic emission (TE) theory, the $\Phi_{bo}(I-V)$ and n were found to depend strongly on temperature, and the n decreases with increasing temperature while the $\Phi_{bo}(I-V)$ increases. The values of Φ_{bo} and n ranged from 0.600 eV and 1.51 (80 K) to 0.816 eV and 1.087 (320 K), respectively. Such behavior of Φ_{bo} and n is attributed to Schottky barrier inhomogeneities by assuming a Gaussian distribution (GD) of BHs at Au/n-GaAs interface. In the calculations, the electrical parameters of the experimental forward bias $I-V$ characteristics of the Au/n-GaAs SBD with the homogeneity in the 80–320 K range have been explained by means of the TE, considering GD of BH with linear bias dependence.

© 2012 Elsevier Ltd. All rights reserved.

1. Introduction

GaAs is a quite versatile semiconductor and the subject of numerous studies owing to its applications in metal–semiconductor (MS) contact, metal–insulator–semiconductor (MIS) structure, metal–insulator–semiconductor field effect transistor (MISFET) devices, light emitting diodes (LEDs) and solar cells [1–5]. Metal deposition on GaAs is a critical process because of the semiconductor's optimum band gap. Also GaAs is known as an ideal material for high efficiency solar cells with a 1.42 eV direct band gap and has large areas of

usage such as optoelectronics, microwave devices and integrated circuits [6,7].

The stability and reproducibility of contact properties and the formation of a high quality Schottky barrier diode (SBD) are essential prerequisites for improvement of device performance. Choosing semiconductor and fabrication methods should be good agreement for the development of device characteristics. Photolithography is a promising technique that allows small diode area with good electrical properties. Since Schottky diode (SD) area is small, it is expected to have low leakage current, low edge related current or smaller defect effects to electrical parameters [8–11].

To understand aspects of current conduction mechanism of the charge carrier transport through MS contact in detail,

* Corresponding author. Tel.: +90 312 2021247; fax: +90 312 212 2279.
E-mail address: dkorucu@yahoo.com (D. Korucu).

the temperature dependence of the I - V characteristics should be investigated in wide temperature range. Surface preparation processes, the interface properties, density of interface states (N_{ss}) at insulator layer/semiconductor interface, series resistance (R_s) of device, thickness of insulator layer at the metal/semiconductor interface and impurity concentration of semiconductor have a dominant influence on the current conduction mechanism and performance and stability of the device [10–20].

According to TE theory, the value of n is expected to be close to unity. But experimental results show that the calculated value of n is greater than unity especially at low temperatures. This case can be attributed to the existence of insulator layer at M/S interface, particular distribution of N_{ss} at semiconductor band-gap and the image force lowering of the barrier [11–18]. Change in the Φ_{bo} and n with changing temperature have been explained on the basis of the TE theory with a GD of the BHs by many researches [18–33]. Biber et. al. [8] have observed that the increase in n and decrease in the Φ_{bo} values with a decrease in temperature in the Au/n-GaAs SDs [18]. The change of n and Φ_{bo} with temperature was explained on the basis of the TE mechanism with GD of the BH by Biber et. al. [8], Bandyopadhyay et. al. [32] and Zhu et. al. [33]. Tung et al. [13] pointed out that the existence of BH inhomogeneities can be explained various anomalous phenomena such as the excess of current at low bias, the anomalous behavior of $n(T)$ and the incomplete saturation of the reverse current [13,14]. Hasegawa et. al. [11] reported properties of micrometer-sized Schottky contacts (SCs) on n-GaAs and n-InP wafers prepared by electrochemical process and lithography technique. They proved that micrometer-sized SBDs are efficient approach to Schottky limit for metal/III-V junctions due to the effects of reducing Fermi level pinning.

In this work, the forward bias current-voltage (I - V) characteristics of the Au/n-GaAs SBDs have been measured in wide temperature ranges of 80–320 K by steps of 10 K. The experimental results of the forward bias I - V measurement show that the values of Φ_{bo} decrease and n increase with decreasing temperature. The temperature dependence of Φ_{bo} and n in Au/n-GaAs SBDs have been interpreted on the basis of the existence of GD of the BHs due to inhomogeneities of the BH at the M/S interface. Photolithography-fabricated Au/n-GaAs SBDs with an area of $3.14 \times 10^{-4} \text{ cm}^2$ were fabricated with a positive photoresist, as discussed below. Many Au/n-GaAs SBDs with the diode diameters ranged from 20 μm to 200 μm were prepared in this technique. However, their forward bias current density (J) vs V characteristics show similar behavior at the intermediate bias range. Therefore, only the results of diode with the area of $3.14 \times 10^{-4} \text{ cm}^2$ corresponding to 200 μm diameter are reported in this paper.

2. Experiment details

The Au/n-GaAs SBDs structure used in this study were fabricated using n-type single crystals n-GaAs wafer with (100) surface orientation, having thickness of 300 μm , 2 in. diameter, 1.2 $\Omega \text{ cm}$ resistivity and $7.3 \times 10^{15} \text{ cm}^{-3}$ carrier concentration (N_D) (given by the manufacturer).

The effective density of states in conduction band (N_C) was taken $4.7 \times 10^{17} \text{ cm}^{-3}$ [1]. Before the SBD fabrication process, n-GaAs wafer was degreased for 5 min in organic solvent of trichloroethylene ($\text{CHCl}_2\text{CHCl}_2$), acetone (CH_3COCH_3) and methyl alcohol (CH_3OH), etched in a sequence of sulfuric acid (H_2SO_4) and hydrogen peroxide (H_2O_2), 20% hydrofluoric acid (HF), a solution of nitric acid (6HNO_3):1HF:35 H_2O , 20% HF and finally quenched in de-ionized water of resistivity of 18 $\text{M}\Omega \text{ cm}$ for a prolonged time. During to each cleaning step, the wafer was rinsed thoroughly in de-ionized water. After surface cleaning of n-GaAs, high purity (99.999%) In with a thickness of about 2000 \AA was coated with at a pressure about 10^{-6} Torr in high vacuum system. To perform the low ohmic contact, n-GaAs wafer was annealed at 425 $^\circ\text{C}$ for 3 min.

For Schottky diode, the n-GaAs wafer was placed on a rotating table. The rotating table was rotated at a fixed rotational speed with 5000 rpm for 45 s using with positive photoresist (AZ5214). Post exposure bake 110 $^\circ\text{C}$ for 50 s. Depending on viscosity of the resist, a certain thickness of film deposited on the n-GaAs wafer. The n-GaAs wafer was rinsed with deionized water then dried with N_2 . After this process UV light was used to cure the resist into the desired structural pattern using a photo mask for 90 s. Develop the exposed resist pattern in MF-701 Developer. The photoresist was then developed 60 s, with the exposed regions dissolving in the solvent. Finally the photoresist was removed for 3 min by acetone and dried with N_2 . Schottky contacts were formed by photolithography process onto the front surface through a photomask of Au dots with 200 μm diameter ($A = 3.14 \times 10^{-4} \text{ cm}^2$).

Current-voltage (I - V) characteristics of Au/n-GaAs SBDs were measured with a Keithley 2400 Sourcemeter and 6514 electrometer. All measurements were carried out at 80–320 K range by steps 10 K using liquid nitrogen (LN) cryostat. Sample temperature controlled by SR 330S with 0.2 K stability during the entire measurements. Current measurement probe with small mass located on the diode by using Newport ESP6000 three axis driver coupled to LN cryostat. A visual basic based program was used for all system control and data collection.

3. Results and discussions

When a SBD with the R_s is considered, according to the TE, it is assumed that the relation between the applied forward bias voltages ($V \geq 3 \text{ kT}/q$) and the current of SBD can be expressed as [1]

$$I = I_o \exp\left(\frac{q(V - IR_s)}{nkT}\right) \left[1 - \exp\left(-\frac{q(V - IR_s)}{kT}\right)\right] \quad (1)$$

where I_o is the reverse-saturation current derived from the linear region of the intercept of $\ln I$ vs V at zero bias, and is given by

$$I_o = AA^*T^2 \exp\left(-\frac{q\Phi_{bo}}{kT}\right) \quad (2)$$

where q , IR_s , n , T , k , A , A^* , Φ_{bo} are electronic charge, voltage drop across R_s of diode, ideality factor, temperature in K, the Boltzmann constant, rectifier contact area, Richardson constant ($8.16 \text{ A/cm}^2 \text{ K}^{-2}$ for n-type GaAs), experimental zero

bias BH (apparent barrier height) of the diode, respectively [1,3]. The forward bias I – V characteristics of Au/n-GaAs SBD fabricated by photolithography technique have been measured in the temperature range of 80–320 K by steps of 10 K, and these $\ln I$ – V characteristics were given in Fig. 1. As can be seen in Fig. 1, there is a deviation from linearity at high forward bias voltages due to the effect of R_s . The values of ideality factor were calculated from the slope of the linear region of the forward bias $\ln I$ – V plots (Fig. 1) for each temperature by using following equation

$$n = \frac{q}{kT} \left(\frac{dV}{d \ln I} \right) \quad (3)$$

The values of I_o were obtained by extrapolating the linear part of $\ln I$ – V plots at intermediate voltage region. Forward bias I – V measurements were made to determine the saturation current I_o from which the zero bias BH Φ_{bo} was defined in terms of the TE theory

$$\Phi_{bo} = \frac{kT}{q} \ln \left(\frac{AA^*}{I_o} \right) \quad (4)$$

The values of Φ_{bo} and n can be determined from intercepts and slopes of the forward bias $\ln I$ – V plot at each temperature using Eqs. (3) and (4), respectively. The obtained Φ_{bo} and n values for each temperature were also given in Table 1. As can be seen in Table 1, the values of Φ_{bo} and n for Au/n-GaAs SBD ranged from 0.600 eV and 1.51 (80 K) to 0.816 eV and 1.087 (320 K), respectively. The high value of n at low temperatures can be attributed to the inhomogeneities of BH, the existence of a thick insulator layer and particular distribution of interface states (N_{ss}) at M/S interface. Moreover, the values of Φ_{bo} and n were found to be strongly temperature dependent. As can be seen from Table 1, Φ_{bo} increases, while n decreases with increasing temperature. The values of n

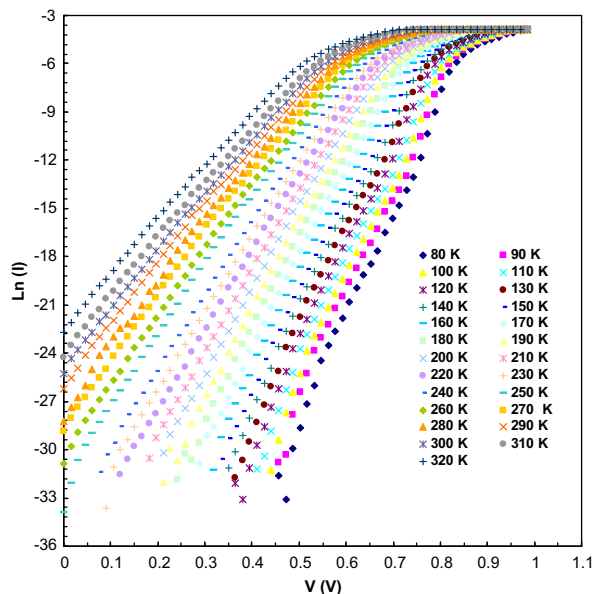


Fig. 1. Forward bias current–voltage (I – V) characteristics of the Au/n-GaAs SBD at various temperature.

Table 1

Temperature dependence of various parameters determined from forward bias I – V characteristics of the Au/n-GaAs SBD in wide temperature range.

T (K)	I_o (A)	n	Φ_{bo} (eV)	$n \cdot \Phi_{bo}$ (eV)	Φ_{bf} (eV)
80	5.02E-36	1.510	0.600	0.906	0.891
90	6.88E-34	1.483	0.616	0.914	0.898
100	3.90E-31	1.451	0.632	0.917	0.900
110	1.54E-28	1.439	0.640	0.921	0.904
120	4.38E-26	1.420	0.642	0.911	0.893
130	5.72E-25	1.383	0.668	0.924	0.906
140	1.68E-23	1.358	0.681	0.924	0.906
150	2.45E-22	1.323	0.696	0.921	0.904
160	5.96E-21	1.317	0.700	0.922	0.904
170	5.76E-20	1.289	0.713	0.919	0.901
180	4.75E-19	1.265	0.724	0.915	0.898
190	3.41E-18	1.243	0.733	0.912	0.895
200	1.78E-17	1.216	0.745	0.906	0.891
210	1.03E-16	1.199	0.752	0.902	0.887
220	4.58E-16	1.176	0.762	0.896	0.882
230	1.93E-15	1.158	0.769	0.891	0.878
240	8.84E-15	1.149	0.773	0.888	0.876
250	3.11E-14	1.131	0.780	0.882	0.871
260	1.25E-13	1.129	0.782	0.883	0.871
270	3.43E-13	1.124	0.790	0.888	0.876
280	1.03E-12	1.119	0.795	0.889	0.877
290	6.96E-12	1.115	0.802	0.886	0.875
300	1.97E-11	1.112	0.808	0.885	0.875
310	4.47E-11	1.094	0.813	0.888	0.878
320	1.08E-10	1.087	0.816	0.887	0.877

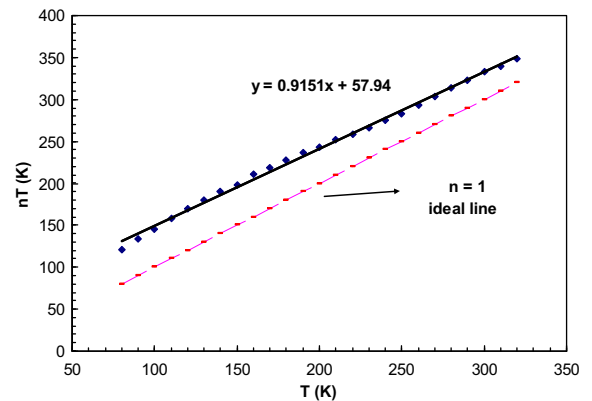


Fig. 2. Plot of nT as a function of T showing the T_o showing the T_o anomaly $n=1+T_o/T$. Also ideal line shows the ideal behavior given as $n=1$.

do not stay constant as the temperature changes. The change in n with temperature, which can be seen in Fig. 2, was found linear with inverse temperature ($1/T$) as following

$$n(T) = n_o + T_o/T \quad (5)$$

where n_o and T_o are constants which were found to be 0.91 and 57.94 K from Fig. 2, respectively. In this case, the temperature dependence of the BH and n of SBD can be called “ T_o effect” or “ T_o anomaly”. It was shown that the T_o effect can be also connected with the lateral inhomogeneity of the BH or the role of the recombination and tunneling current components [14–18,28]. Fig. 2 shows

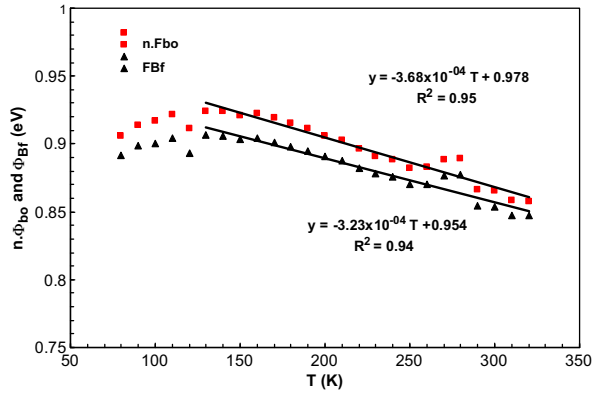


Fig. 3. Flat band BH as a function of temperature. The continuous line represents the best fit to the points in wide temperature ranges.

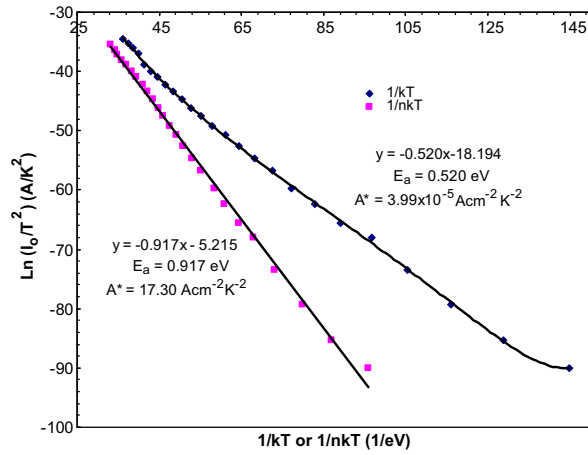


Fig. 4. Richardson plots of the $\ln(I_o/T^2)$ vs $1/T$ or $1/nT$ for Au/n-GaAs SBD.

that the nT versus T plot reporting the temperature dependence of n , in which the ideal line give the ideal behavior of a SC, i.e., with $n=1$. In this behavior, the straight line fitted to the experimental values for the T_o effect should be parallel to that of the ideal SC behavior [3,13]. In order to explain the change in n with temperature, various mechanisms which take the density distribution of N_{ss} , quantum mechanical tunneling and image force lowering into account have been proposed in literature [34–45].

Sometimes, the obtained experimental BH is called the apparent BH or the zero-bias barrier height (Φ_{bo}). The BH obtained under flat band condition is called the flat band BH (Φ_{bf}) and is considered as the real essential quantity. The flat band BH Φ_{bf} can be calculated using the experimental n and zero bias BH (Φ_{bo}) according to Eq. (6). Thus the real or flat band BH (Φ_{bf}) can be expressed as [1,35]

$$\Phi_{bf} = n\Phi_{bo} - (n-1) \frac{kT}{q} \ln\left(\frac{N_C}{N_D}\right) \quad (6)$$

where N_C is the density of states in the conduction band and N_D is the doping concentration in the semiconductor. Here, the values of N_D and N_C were taken as

$7.3 \times 10^{15} \text{ cm}^{-3}$, $4.7 \times 10^{17} \text{ cm}^{-3}$, respectively, and their values were assumed to stay constant with temperature.

Thus, the temperature dependence of Φ_{bf} was calculated from Eq. (6) and obtained values were given in Table 1. As can be seen in Fig. 3, the values of Φ_{bf} change linearly with temperature as

$$\Phi_{bf}(T) = \Phi_{bf}(T=0) + \alpha T \quad (7)$$

where $\Phi_{bf}(T=0)$ is the flat-band BH extrapolated to zero temperature and α is the temperature coefficient of $\Phi_{bf}(T)$. Fig. 3 shows the variation of $n\Phi_{bo}$ and Φ_{bf} as a function of temperature. It is evident that the values of $(n\Phi_{bo})$ and Φ_{bf} are larger than Φ_{bo} especially at low temperatures. However, they approach to Φ_{bo} at high temperatures. As can be seen in Fig. 3, the fitting of $(n\Phi_{bo})$ and Φ_{bf} data in Eq. (7) yield $n\Phi_{bo}(T=0)$, 0.978 eV and $\alpha = -3.68 \times 10^{-4} \text{ eV K}^{-1}$ and $\Phi_{bf}(T=0)$, 0.954 eV and $\alpha = -3.23 \times 10^{-4} \text{ eV K}^{-1}$ in wide temperature ranges of 130–320 K, respectively. It is clear that these values are close to their theoretical value of negative temperature coefficient (α) of band gap for GaAs ($5.405 \times 10^{-4} \text{ eV K}^{-1}$) [1].

In order to evaluate the BH in another way, we use the Richardson plot of the reverse saturation current I_o . By taking the natural logarithm of Eq. (2), can be rewritten as

$$\ln\left(\frac{I_o}{T^2}\right) = \ln(AA^*) - \frac{q\Phi_{bo}}{kT} \quad (8)$$

The $\ln(I_o/T^2)$ vs q/kT and $\ln(I_o/T^2)$ vs q/nkT plots were given in Fig. 4. As can be seen in Fig. 4, the $\ln(I_o/T^2)$ vs q/nkT plot is linear rather than the conventional Richardson plot of $\ln(I_o/T^2)$ vs q/kT . Activation energy (E_a) and Richardson constant (A^*) values were obtained from the slope and intercept at an ordinate of the linear region of the $\ln(I_o/T^2)$ vs q/kT plot as 0.520 eV, $3.99 \times 10^{-5} \text{ A cm}^{-2} \text{ K}^{-2}$ and $\ln(I_o/T^2)$ vs q/nkT plot as 0.917 eV, $17.30 \text{ A cm}^{-2} \text{ K}^{-2}$, respectively. The value of A^* calculated from $\ln(I_o/T^2)$ vs q/nkT plot is much lower than the known value of $8.16 \text{ A cm}^{-2} \text{ K}^{-2}$ for electrons in n-GaAs. Also the value of E_a obtained from $\ln(I_o/T^2)$ vs q/kT is almost equal to the half of the forbidden band gap of n-GaAs. On the other hand the values of E_a obtained from $\ln(I_o/T^2)$ vs q/nkT is almost the forbidden band gap and the

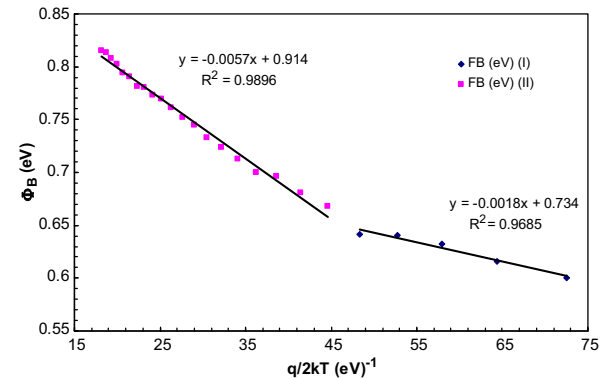


Fig. 5. Experimental BH Φ_{bo} (I - V) vs $q/2kT$ plots for Au/n-GaAs SBD.

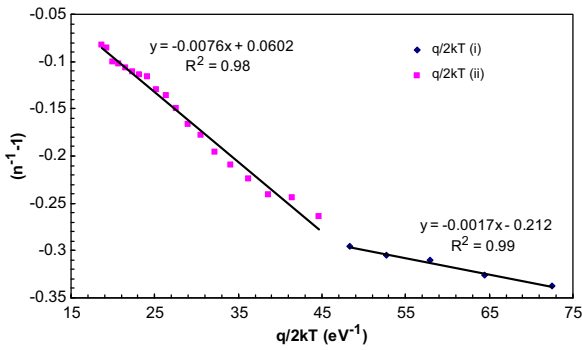


Fig. 6. Experimental ideality factor ($n^{-1}-1$) vs $q/2kT$ plot for Au/n-GaAs SBD.

value of A^* obtained from $\ln(I_0/T^2)$ vs q/nkT is close to theoretical value of $8.16 \text{ A cm}^{-2} \text{ K}^{-2}$ for electrons in n-GaAs. When the temperature is lowered, Φ_{bo} decreased, n increased and the Richardson plot deviated from linearity. These variations with temperature can be explained by the influence of the Schottky barrier inhomogeneities [41].

The commonly observed deviation from classical TE theory, as will be discussed below, can be explained by a recent model based on the assumption of a spatial fluctuation of the BH at interface. If the BH has GD with the zero bias mean BH $\Phi_{ap}(\approx \bar{\Phi}_{Bo})$ and standard deviation σ_o , the GD of the BHs yields the following expression of the BH as [1,34]

$$\Phi_{ap} = \bar{\Phi}_{Bo}(T=0) - \frac{q\sigma_o}{2kT} \quad (9)$$

where the temperature dependence of σ_o is usually small and can be neglected [33]. The observed variation of n with temperature in the model is given by

$$\left(\frac{1}{n_{ap}} - 1\right) = \rho_2 - \frac{q\rho_3}{2kT} \quad (10)$$

where n_{ap} is apparent ideality factor and ρ_2 and ρ_3 are voltage coefficients which may depend on temperature, quantifying the voltage deformation of the BH distribution [28,42–45].

The necessary parameters to draw the temperature dependent theoretical I – V characteristics considering the bias dependence of BHs in the distribution though mean BHs in inhomogeneous SDs have been obtained from the experimental Φ_{bo} vs $q/2kT$ (Fig. 5) and n_{ap} vs $q/2kT$ (Fig. 6) plots drawn by means of the temperature dependent I – V data of the Au/n-GaAs SC fabricated by photolithography. These plots respond to two lines instead of a single straight line with transition occurring at 130 K. The intercept and slope of the straight line have given two sets of values of Φ_{bo} and σ_o as 0.914 eV and 0.00285 V in the temperature range of 130–320 K, and 0.734 eV and 0.009 V in the temperature range of 80–120 K. The values of ρ_2 obtained from the intercepts of the experimental n_{ap} versus $1/T$ plot are -0.0602 in the 130–320 K range and 0.212 in the 80–120 K range, whereas the values of ρ_3 from the slopes are -0.0076 V in the 130–320 K range and -0.0017 V in the 80–120 K.

As explained above the value of A^* was found changeable according to used method. Experimental results show that the extracted value of the A^* has been found to be several orders of magnitude lower than the theoretical value. Also, the obtained value of A^* may be different depending on used calculation method. This discrepancy between the experimental and theoretical values of A^* was reported by many researchers in the last years [8,13–26]. Such fluctuation in A^* can be attributed to the spatial inhomogeneous BH and potential fluctuations at the interface, that consist of low and high barrier areas, that is, the current transport mechanism across diode would flow preferentially through the lower barriers in the potential distribution. As explained by Horvath [26], the value of A^* obtained from the temperature dependence of the forward bias I – V characteristics may be effected by lateral inhomogeneity of the barrier. Therefore, the lower value of experimentally determined A^* indicates that the effective active area is in fact much smaller than the diode rectifier contact area [18–29]. As temperature increase, the lower BH of the patches at MS interface is offset by the much greater area of the uniform region, as a result, most current flows through the uniform region.

4. Conclusion

The forward bias I – V characteristics of the Au/n-GaAs SBD were measured in the temperature range of 80–320 K. The evaluation of the experimental forward bias I – V characteristics with TE mechanism shows an increase of Φ_{bo} and a decrease of n with increasing temperature. By using the TE theory, the $\Phi_{bo}(I$ – $V)$ and n were found to depend strongly on temperature and the n decreases with increasing temperature while the $\Phi_{bo}(I$ – $V)$ increases. The values of Φ_{bo} and n ranged from 0.600 eV and 1.51(80 K) to 0.816 eV and 1.087 (320 K), respectively. This behavior of $\Phi_{bo}(I$ – $V)$ is an obvious disagreement with the reported negative temperature coefficient of the BH. This change of $\Phi_{bo}(I$ – $V)$ and n is attributed to Schottky barrier inhomogeneities by assuming GD of BHs due to barrier inhomogeneities that prevails at M/S interface. Φ_{bo} vs $q/2kT$ plot was drawn to obtain evidence of GS of the BHs. The intercept and slope of the straight line have given two sets of values of Φ_{bo} and σ_o as 0.914 eV and 0.00285 in the temperature range of 130–320 K, and 0.734 eV and 0.009 V in the temperature range of 80–120 K. In summary, the temperature dependence of the forward I – V characteristics of the Au/n-GaAs SBD can be successfully explained on the basis of TE mechanism with GD of the BHs.

Acknowledgments

This work is supported by Tubitak and Author also thanks to Dr. R. Airey for diode fabrication in Sheffield University EPSRC Centre.

References

- [1] S.M. Sze, *Physics Semiconductor Devices*, John Wiley and Sons, New York, 1981, pp. 24–30.

- [2] Y.P. Song, R.L. Van Meirhaeghe, W.H. Laflere, F. Cardon, *Solid-State Electronics* 29 (1986) 663–668.
- [3] M.K. Hudait, P. Venkateswarlu, S.B. Krupanidhi, *Solid State Electronics* 45 (2001) 133–141.
- [4] F. Chekir, G.N. Lu, C. Barret, *Solid State Electronics* 29 (1986) 519–522.
- [5] V.W.L. Chin, M.A. Green, J.W.V. Storey, *Journal of Applied Physics* 68 (1990) 3470–3474.
- [6] T.S. Huang, R.S. Fang, *Solid State Electronics* 37 (1994) 1652–1661.
- [7] M. Didio, A. Cola, M.G. Lupo, L. Vasanelli, *Solid-State Electronics* 38 (1995) 1923–1928.
- [8] M. Biber, C. Coskun, A. Turut, *European Physical Journal Applied Physics* 31 (2005) 79–86.
- [9] W.I. Park, Gyu-Chul Yia, J.-W. Kim, S.-M. Park, *Applied Physics Letters* 82 (2005) 24–30.
- [10] D. Korucu, T.S. Mammadov, S. Özcelik, *Journal of Ovonic Research* 4 (2008) 159–164.
- [11] H. Hasegawa, T. Sato, C. Kaneshiro, *Journal of Vacuum Science and Technology B* 17 (1999) 1856–1866.
- [12] P. Chattopadhyay, A.N. Daw, *Solid-State Electronics* 29 (1986) 555–560.
- [13] R.T. Tung, *Physical Review B* 45 (1992) 13509–13523.
- [14] K. Ejderha, A. Zengin, I. Orak, B. Tasyurek, T. Kilinc, A. Turut, *Materials Science in Semiconductor Processing* 14 (2011) 5–12.
- [15] O. Gullu, M. Biber, R.L. Van Meirhaeghe, A. Turut, *Thin Solid Films* 516 (2008) 7851–7856.
- [16] J.H. Werner, H.H. Güttler, *Journal of Applied Physics* 69 (1991) 1522–1533.
- [17] S. Chand, S. Bala, *Applied Surface Science* 252 (2005) 358–363.
- [18] S. Duman, B. Gurbulak, A. Turut, *Applied Surface Science* 253 (2007) 3899–3905.
- [19] A.F. Ozdemir, A. Turut, A. Kokce, *Semiconductor Science and Technology* 21 (2006) 298–302.
- [20] M. Biber, O. Gullu, S. Forment, R.L. Van Meirhaeghe, A. Turut, *Semiconductor Science and Technology* 21 (2006) 1–5.
- [21] M.K. Hudait, S.B. Krupanidhi, *Physica B* 307 (2001) 125–137.
- [22] W.P. Leroy, K. Opsomer, S. Forment, R.L. Van Meirhaeghe, *Solid State Electronics* 49 (2005) 878–883.
- [23] H. Altuntas, S. Altindal, H. Shtrikman, S. Ozcelik, *Microelectronics Reliability* 49 (2009) 904–911.
- [24] O. Vural, Y. Safak, S. Altindal, A. Turut, *Current Applied Physics* 10 (2010) 761–765.
- [25] W. Mönch, *Journal of Vacuum Science and Technology B* 17 (1999) 1867–1876.
- [26] Zs.J. Horvath, *Solid-State Electronics* 39 (1996) 176–181.
- [27] O. Demircioglu, S. Karatas, N. Yildirim, O.F. Bakkaloglu, A. Turut, *Journal of Alloys and Compounds* 509 (2011) 6433–6439.
- [28] Ş. Karatas, Ş. Altindal, A. Türüt, A. Özmen, *Applied Surface Science* 217 (2003) 250–260.
- [29] W.C. Huang, C.T. Horng, *Applied Surface Science* 257 (2011) 3565–3569.
- [30] R. Sharma, *Journal of Electron Devices* 8 (2010) 286–292.
- [31] N. Yildirim, A. Turut, V. Turut, *Microelectronic Engineering* 87 (2010) 2225–2229.
- [32] S. Bandyopadhyay, A. Bhattacharyya, S.K. Sen, *Journal of Applied Physics* 85 (1999) 3671–3676.
- [33] S. Zhu, R.L. Van Meirhaeghe, C. Detavernier, F. Cardon, G.P. Ru, X.P. Qu, et al., *Solid State Electronics* 44 (2000) 663–669.
- [34] H. Korkut, N. Yildirim, A. Turut, H. Dogan, *Materials Science and Engineering B* 157 (2009) 48–52.
- [35] S. Dogan, S. Duman, B. Gurbulak, S. Tuzemen, H. Morkoc, *Physica E* 41 (2009) 646–651.
- [36] N. Yildirim, A. Turut, *Microelectronic Engineering* 86 (2009) 2270–2274.
- [37] T. Goksu, N. Yildirim, H. Korkut, A.F. Ozdemir, A. Turut, A. Kokce, *Microelectronic Engineering* 87 (2010) 1781–1784.
- [38] D. Korucu, *Journal of Optoelectronics and Advanced Materials* 12 (2010) 2194–2198.
- [39] D. Korucu, *Journal of Optoelectronics and Advanced Materials* 14 (2012) 41–48.
- [40] M. Gulnazar, H. Efeoglu, *Solid-State Electronics* 53 (2009) 972–979.
- [41] Y. Gulen, M. Alanyalioglu, K. Ejderha, *Journal of Alloys and Compounds* 509 (2011) 3135–3159.
- [42] J. Osvald, Zs.J. Horvath, *Applied Surface Science* 234 (2004) 349–354.
- [43] H. Korkut, N. Yildirim, A. Turut, *Physica B* 404 (2009) 4039–4044.
- [44] S. Asubay, O. Gullu, B. Abay, A. Turut, A. Yilmaz, *Semiconductor Science and Technology* 23 (2008) 035006–0365012.